

Journal of Materials Chemistry B

Accepted Manuscript



This is an *Accepted Manuscript*, which has been through the Royal Society of Chemistry peer review process and has been accepted for publication.

Accepted Manuscripts are published online shortly after acceptance, before technical editing, formatting and proof reading. Using this free service, authors can make their results available to the community, in citable form, before we publish the edited article. We will replace this *Accepted Manuscript* with the edited and formatted *Advance Article* as soon as it is available.

You can find more information about *Accepted Manuscripts* in the [Information for Authors](#).

Please note that technical editing may introduce minor changes to the text and/or graphics, which may alter content. The journal's standard [Terms & Conditions](#) and the [Ethical guidelines](#) still apply. In no event shall the Royal Society of Chemistry be held responsible for any errors or omissions in this *Accepted Manuscript* or any consequences arising from the use of any information it contains.

Supercritical carbon dioxide-assisted drug loading and release
from biocompatible porous metal-organic frameworks

Kiyoshi Matsuyama^{a,*}, *Nobukatsu Hayashi*^a, *Misaki Yokomizo*^a, *Takafumi Kato*^b,

Kiyomi Ohara^b, *Tetsuya Okuyama*^c

^a Department of Biochemistry and Applied Chemistry, Kurume National College of
Technology, 1-1-1 Komorino, Kurume, Fukuoka 830-8555, Japan

^b Department of Chemical Engineering, Fukuoka University, 8-19-1 Nanakuma Jonan-ku,
Fukuoka 814-0180, Japan

^c Department of Materials Science and Engineering, Kurume National College of Technology,
1-1-1 Komorino, Kurume, Fukuoka 830-8555, Japan

* Corresponding author

Kiyoshi Matsuyama

E-mail address: mtym@kurume-nct.ac.jp

Telephone +81-942-35-9403

Fax +81-942-35-9400

ABSTRACT

Herein we describe the supercritical carbon dioxide (scCO₂)-assisted drug loading and release from nontoxic and biocompatible porous iron (III) polycarboxylate metal-organic frameworks (MOFs), which exhibited very high cargo loadings and gradual release. MIL-53(Fe) and MIL-100(Fe) were investigated as potential carriers for drug molecules, using ibuprofen as a model drug candidate. The loading and release behaviour of ibuprofen were monitored by thermogravimetric analyses (TGA) and high performance liquid chromatography (HPLC) measurements to quantitatively determine the ibuprofen uptake, and have been performed for the first time using scCO₂-based technology. After the preparation of the MOFs within a particular solvent, the internal surface area of MIL-53(Fe) and MIL-100(Fe) increased as a result of the scCO₂ drying method. Furthermore, ibuprofen could be impregnated into the pores of the MOFs by utilizing a scCO₂-hexane solution. ScCO₂-assisted impregnation could also be used to deliver ibuprofen to the pores of the MOFs. As a result, a large amount of ibuprofen was able to be loaded into MIL-53(Fe) and MIL-100(Fe).

KEYWORDS: Metal-Organic Framework, Supercritical Carbon Dioxide, Drug Delivery, Impregnation, Ibuprofen

Introduction

Well-designed metal-organic hybrid porous materials such as metal-organic frameworks (MOFs) or porous coordination polymers (PCPs) can be made by connecting various organic linkers with metal ions. This class of materials was recently recognized as an intriguing class of crystalline nanoporous materials with potential applications in gas storage, separation, catalysis, and more recently biomedicine.¹⁻⁶ The high and regular porosity of MOFs combined with their amphiphilic internal microenvironment have facilitated the achievement of record drug loadings and controlled release.⁷⁻¹⁰ Recently, a new form of controlled drug delivery system that utilizes non-toxic and biodegradable porous iron (III) polycarboxylate MOFs has been developed and exhibited very high cargo loadings and gradual controlled release.¹¹⁻¹⁴ These results indicate that MOFs possess significant advantages over conventional drug delivery systems in obtaining high drug loadings and facile controlled release kinetics. Horcajada *et al.* demonstrated that specific non-toxic porous iron (III)-based MOFs with well-defined cores and surfaces, in addition to imaging properties, can function as superior nanocarriers for efficient controlled delivery of complex antitumoural and retroviral drugs against cancer and AIDS.¹² Furthermore, the loading and release behaviour of caffeine and ibuprofen from iron (III)-based MOFs such as MIL-53, MIL-88, MIL-100, MIL-101, and MIL-127 have been thoroughly investigated both experimentally and computationally.^{13, 15, 16} Although MOFs exhibit a large pore volume for drug loading, it is difficult to completely occupy the pores of the MOFs with drugs. Recently, Liedana *et al.* have succeeded in the one-step encapsulation of caffeine in NH₂-MIL-88B(Fe), which demonstrated high guest loading and controlled release.¹⁷ In their investigation, caffeine was added to the synthetic solution of the MOF such that the MOF structure was formed around the caffeine itself.

The material properties of MOFs and PCPs that make them attractive for various applications are their permanent microporosities and large internal surface areas. For example, MOFs and PCPs possess controllable pore geometries that have demonstrated record-breaking surface areas (pore volume) and desirable gas-storage performances.^{18, 19} Unfortunately, the surface areas attained experimentally are often less than those predicted from computational studies or single-crystal X-ray structural studies.^{15, 20} Typically, MOFs and PCPs are prepared in solution and the solvent needs to be removed to allow guest molecules to enter the pores. Although the solvent can be directly removed by heating under reduced pressure, the network-forming bonds may break and block the channels. Furthermore, the loss of the solvent can also create a capillary pressure at the liquid–vapour interface of the solvent (surface tension) and subsequently force the pores to collapse. In order to overcome these challenges, a drying procedure that utilizes supercritical carbon

dioxide (scCO₂) may be used to improve the pore stabilities of the MOFs and PCPs. The scCO₂ drying procedure has been previously employed with porous and nanostructured materials.^{21,22} A drying procedure that uses scCO₂ provides greater access to the pores of the PCPs and MOFs and subsequently produces larger internal surface areas.²³⁻³⁰ ScCO₂ is the solvent of choice for a variety of applications because it is readily available, inexpensive, and environmentally benign. ScCO₂ offers specific advantages for the formation of porous materials because it has a low viscosity and high diffusivity and will never condense into a liquid above the critical temperature. Furthermore, the impregnation technique utilizing scCO₂ is an effective approach to uniformly decorating and impregnating porous materials.^{22,31-34} ScCO₂ is expected to overcome the limitations of diffusivity and mass transfer of conventional solvents and is capable of introducing effective significant amount of target materials into the pores of the MOFs. Recently, Zhao *et al.* reported the immobilization of ruthenium nanoparticles on MOF nanorods using a scCO₂-methanol solution to produce a highly efficient catalyst.³⁵ ScCO₂-assisted drying and impregnation procedures may be an effective method for obtaining a high loading of medicine in the pores of iron (III) polycarboxylate MOFs.

The objectives of this study were to develop scCO₂-assisted drug loading and release from nontoxic and biocompatible porous iron (III) polycarboxylate MOFs with very high loadings and a gradual release. Additionally, we investigated the effects of several experimental conditions on the drug loading ratio and drug release behaviour of the MOFs.

Results and discussion

ScCO₂ drying of MOFs

Before conducting the experiments regarding the drug loading and release from the MOFs, we attempted scCO₂ drying of MIL-53(Fe) and MIL-100(Fe) to obtain dry samples. A drying procedure that utilizes scCO₂ provides greater access to the pores of the MOFs, which then produces larger internal surface areas. The larger surface areas of the MOFs could then yield higher loading capacities of drug molecules within MOFs. Prior to the drying of the MOFs, the solvent remaining from the MOF synthesis was first exchanged with ethanol. We selected ethanol as the exchange solvent because it is miscible with CO₂.³⁶ ScCO₂ drying of the MOFs was carried out at 20 MPa and 353 K for 6 h. For the MOF samples obtained by conventional drying, the MOF particles were dried at 353 K under reduced pressure.

SEM and optical photographs of MIL-53(Fe) and MIL-100(Fe) prepared using scCO₂ and conventional drying are shown in Fig.1, while the mean particle sizes, BET surface

areas, and pore volumes are summarized in Table 1. The particle sizes of MIL-53(Fe) and MIL-100(Fe) prepared by scCO₂ drying were 0.77 μm and 0.34 μm, respectively. However, aggregated particles were obtained by the conventional drying method under reduced pressure at 353 K. N₂ isotherms of MIL-53(Fe) and MIL-100(Fe) are also shown in Fig.2. The N₂-accessible surface areas of MIL-53(Fe) and MIL-100(Fe) prepared by conventional drying were 57 m²•g⁻¹ and 1230 m²•g⁻¹, respectively. For the samples subjected to scCO₂ drying, the N₂-accessible surface areas increased to 990 m²•g⁻¹ for MIL-53(Fe) (a 17-fold increase) and 1500 m²•g⁻¹ for MIL-100(Fe) (a 1.2-fold increase). ScCO₂ drying prevents the aggregation of MOF particles and the collapse of MOF pores caused by the capillary pressure at the liquid-vapour interface of solvent during the conventional solvent evacuation process. For the samples subjected to scCO₂ drying, the remaining solvent within the pores was readily separated by simple depressurization, without capillary pressure. The XRD patterns of dried MIL-53(Fe) and MIL-100(Fe) are shown in Fig.3. The crystal structure of MIL-53(Fe) and MIL-100(Fe) was not dependent on the drying process. Nelson *et al.* reported the significant enhancement of the surface areas of MOFs by scCO₂ drying, as well as the decreased surface area caused by the misalignment of the micropores at the particle-particle boundaries of the MOFs inhibiting the access of N₂ gas molecules to the internal microporous surfaces of the MOF upon the evacuation of the solvent.²⁶

ScCO₂-Assisted Drug Loading

In order to obtain a higher loading of ibuprofen onto MIL-53(Fe) and MIL-100(Fe), scCO₂ impregnation was carried out. The loading ratios of ibuprofen on MIL-53(Fe) and MIL-100(Fe) were determined by TGA analysis. The TGA data are shown in Fig. 4 and Fig. 5 while the loading ratios of ibuprofen are summarized in Table 2. In order to check the reliability of TGA measurement for the determination of loading ratios of ibuprofen in MOFs, the ibuprofen amount content was also estimated by XRF, elemental analysis, and high performance liquid chromatography (HPLC) in previous work.¹⁶ In this work, ibuprofen contents were also determined by HPLC, and the elemental analysis using electron probe microanalyzer (EPMA) equipped with a wavelength dispersive X-ray spectrometer (WDX). The reliable loading ratios were obtained by TGA, EPMA elemental analysis, and HPLC analysis as shown in Table 2. The details of experimental results for EPMA elemental analysis are shown in supporting information (Tables S1 – S3). The experimental data of ibuprofen loading ratio determined by HPLC in Table 2 were actual ibuprofen loading ratio calculated from the HPLC data. Taking into account the ibuprofen content obtained by the different techniques (TGA, elemental analysis, and HPLC analysis), the obtained experimental data based on TGA are reliable. For the conventional impregnation of ibuprofen with hexane, the

ibuprofen loading ratio on MIL-53(Fe) prepared with scCO₂ drying and conventional drying were 15.5 wt.% and 13.2 wt.%, respectively. Horcajada *et al.* reported similar loading ratios of ibuprofen using conventional impregnation with hexane.¹³ The Loading ratio is 0.210 [g-ibuprofen/g-dehydrated MIL-53(Fe)] (the value of drug loading ratio is 17.4 wt.%). However, Horcajada *et al.* also reports the values of 22 wt.% for MIL-53(Fe) and 33 wt.% for MIL-100(Fe) for conventional loading.¹² These difference results are due to the experimental impregnation condition such as solvent. The loading ratio of target substance in MOF is strong depended on the nature of solvent (e.g., hydrophilic and hydrophobic properties). In order to indicate the effect of scCO₂ on the enhancement of the loading ration ibuprofen into MOF pores, we use hexane as conventional impregnation solvent in this work. Although the surface area and pore volume of MIL-100(Fe) were higher than those of MIL-53(Fe), the ibuprofen loading ratios on MIL-100(Fe) prepared with scCO₂ drying and conventional drying were 9.1 wt.% and 6.9 wt.%, respectively. The ibuprofen loading ratio on MIL-53(Fe) by conventional impregnation with hexane was lower than that on MIL-100(Fe). These results could be attributed to the crystal structures of MIL-53(Fe) and MIL-100(Fe). Although MIL-53(Fe) exhibits a three-dimensional structure with a microporous 1D pore system¹³, MIL-100(Fe) contains two forms of mesocages (25 Å and 29 Å) accessible through microporous windows (~4.7 Å × 5.5 Å and 8.6 Å).³⁷ For the impregnation of ibuprofen using hexane, the complex pore structure of MIL-100(Fe) inhibited the loading of ibuprofen within the micropores. The ibuprofen will be preferentially adsorbed only within the larger cages. The minimal amount of ibuprofen dissolved in hexane was not sufficient to be introduced into the micropores of MIL-100(Fe).

In this investigation, we utilized scCO₂-assisted ibuprofen loading to increase the loading of ibuprofen on MOFs. Prior to the scCO₂-assisted ibuprofen loading experiment, MIL-53(Fe) and MIL-100(Fe) were dried with scCO₂. The loading ratios of ibuprofen on MIL-53(Fe) and MIL-100(Fe) were 31.3 wt.% and 41.7 wt.%, respectively (see Fig. 4). Ibuprofen molecules fill with cavities of MIL-53(Fe) and MIL-100(Fe), because ibuprofen delivered from MOFs within 1 d. When ibuprofen molecules did not fill with cavities of MOFs, ibuprofen was completely delivered from MOFs within 30 min. Release behaviour of ibuprofen from MOFs was described at later section. The loading ratio of MIL-100(Fe) was higher than that of MIL-53(Fe) because MIL-100(Fe) had a larger pore volume. The ScCO₂-assisted method dramatically enhanced the loading ratio of ibuprofen because scCO₂ accelerated the penetration of ibuprofen into mesopores and micropores of the MOFs. High diffusivity and low viscosity of scCO₂ achieve the transfer of an effective amount of target materials into pores of MOFs. Wakayama *et al.* reported that scCO₂ could be used to synthesize nanoparticles within microporous or mesoporous silicas exhibiting uniform pore

sizes, such as FSM-16 (1.6-3.5 nm in diameter).³¹ The nanoparticles could be impregnated into the micropores and mesopores of FSM-16 by utilizing a supercritical fluid. Alternatively, nanoparticles could not be introduced into the smaller pores of FSM-16 by impregnation using conventional liquid solvents as a result of the difference in penetration into the nanoporous structures between scCO₂ and conventional liquid solvents. In this study, mixtures of scCO₂ and conventional solvents (hexane) were used as the impregnation solvent because the solubility of CO₂-expanded liquids and scCO₂ augmented with a co-solvent was significantly more customizable than those of scCO₂.³⁸ Although the solubility of ibuprofen in scCO₂ was 4.23×10^{-3} (mole fraction) at 200 bar and 40°C³⁹, the solubility of ibuprofen in CO₂-organic solvent was 0.1 (mol drug per mol solvent).⁴⁰ Hillerström *et al.* confirmed that ibuprofen can be loaded into mesoporous silica using liquid (near-critical) CO₂ as the solvent.⁴¹ The scCO₂-hexane mixtures can therefore transfer an effective amount of ibuprofen into the pores of MOFs. In order to indicate the advantage of scCO₂ assisted drug loading, we try to the scCO₂ assisted drug loading without drying of MOF (one-step drug loading). The loading ratio of ibuprofen on MIL-53(Fe) was 9.0 wt.% and its value is very low (see the supporting information (Fig. S1)). The drying procedure is the important process to achieve the activation of MOFs and the higher loading ratio of ibuprofen in MOFs.

The interactions between ibuprofen and the pores of the MOFs were evaluated by TGA and FT-IR. As shown in Fig. 4(a-2) and Fig. 5(a-2), the decomposition of pristine ibuprofen was observed in the range of 150-190°C. The weight loss in the range of 300-350°C corresponded to the destruction of pristine MIL-53(Fe) (Fig. 4(a-2)). The destruction of ibuprofen within ibuprofen-loaded MIL-53(Fe) occurred in the range of 150-250°C (Fig. 4(b) through Fig. 4(d)). The destruction temperature of ibuprofen within MIL-53(Fe) was higher than that of pure ibuprofen. Similar destruction behaviour was also observed for MIL-100(Fe), as shown in Fig. 5(b) through Fig. 5(d). These results were attributed to the small pore sizes of MIL-53(Fe) and MIL-100(Fe) (8Å and 25-29 Å, respectively) as well as stronger interactions between the ibuprofen and the MOF matrix. As shown in Fig. 6, the FT-IR spectra confirmed the incorporation of ibuprofen during the loading process. The loaded ibuprofen within the MOF matrix was confirmed by the C-H stretching band at 2994 cm⁻¹ and the -O-C-O- vibration bands around 1430 and 1550 cm⁻¹. Furthermore, the C=O stretching band of pristine ibuprofen at 1722 cm⁻¹ shifted to lower wavelengths (1698 cm⁻¹) upon incorporation into the MOFs, which was indicative of the formation of hydrogen bonds between the carboxylic group of ibuprofen and hydroxyl groups of MIL-53(Fe) (Fig. 6(c)). Similar behaviours were reported for the conventional loading of ibuprofen with hexane¹³ and the conventional loading of caffeine with ethanol.¹⁶

Release behaviour of ibuprofen from MIL-53(Fe) and MIL-100(Fe)

The ibuprofen-loaded MIL-53(Fe) and MIL-100(Fe) were first compacted into cylindrical pieces. The delivery of ibuprofen was performed in PBS and the amount of released ibuprofen was quantified by HPLC. Ibuprofen was completely delivered from MIL-53(Fe) and MIL-100(Fe) within 1 d, as shown in Fig. 7 and Fig. 8, respectively. The 100% release value on in Figures 7 and 8 is experimental value where no more ibuprofen release was observed. Ibuprofen delivery was relatively fast in PBS compared to the release behaviour into simulated body fluids.¹³ In the simulated body fluids, slow delivery of the cargo molecules was observed and was completed after 3 weeks. In this investigation, the degradation of framework caused by PBS governs the release of ibuprofen as a result of framework collapse of the metal polycarboxylate MOFs within the PBS medium. PBS accelerates the degradation of the framework of the MIL-53(Fe) and MIL-100(Fe). Details regarding the degradation behaviour of MIL-53(Fe) and MIL-100(Fe) have been reported by Cunha *et al.*¹⁶ Framework degradation due to the replacement of the carboxylate linkers by phosphate groups occurred in PBS. Alternatively, higher release amounts of ibuprofen were obtained by the *scCO*₂-assisted loading of ibuprofen on MIL-53(Fe) and MIL-100(Fe) because higher loading amounts of ibuprofen within the pores of the MOFs were achieved.

Experimental

Preparation of MIL-53(Fe) and MIL-100(Fe)

In this investigation, MIL-53(Fe) and MIL-100(Fe) were used as porous iron (III)-based MOFs, and were synthesized as follows. The details of the synthetic methodology have been described in previous studies.^{13, 37} MIL-53(Fe) was synthesized from a mixture of $\text{FeCl}_3 \cdot 6\text{H}_2\text{O}$, terephthalic acid, and *N,N*'-dimethylformamide (DMF) at a molar ratio of 1:1:280 using a Teflon-lined autoclave where the mixture was heated for 15 h at 150°C. A yellow powder corresponding to the MIL-53(Fe) solid containing DMF within the pores was obtained by filtration. MIL-100(Fe) was synthesized from a mixture of $\text{FeCl}_3 \cdot 6\text{H}_2\text{O}$, trimesic acid, hydrofluoric acid, HNO_3 , and water at a molar ratio of 1:0.66:2.0:1.2:280 using a Teflon-lined autoclave where the mixture was heated for 6 d at 150°C. The light-orange powder was recovered by filtration and washed with water.

The prepared MIL-53(Fe) and MIL-100(Fe) were then evacuated with *scCO*₂. Prior to *scCO*₂ drying, the washed MOF samples were soaked in absolute ethanol, replacing the solvent every 24 h for 72 h, to exchange the occluded solvent for ethanol. The

ethanol-containing samples were then placed in a high-pressure cell (50 cm³). In order to exchange ethanol with CO₂, CO₂ was pumped into the high-pressure cell for 6 h through a pre-heater at pressures and temperatures as high as 20 MPa and 353 K. The flow rate of CO₂ was 2.0 ml•min⁻¹. The cell was then placed within an air bath and the system temperature was maintained at 353±0.1 K. The system pressure was also set to 20 MPa using a backpressure regulator. After the scCO₂ drying procedure, the vessel was slowly depressurized to atmospheric pressure for approximately 30 min and the samples were removed. The system temperature was maintained at 353 K (above the critical temperature of CO₂, 304.2 K) to prevent the formation of the liquid–vapour interface upon depressurization because the capillary pressure at the liquid–vapour interface would accelerate the collapse of pores of the MOFs.

Incorporation of ibuprofen

0.5 g of the dried MOF and 0.5 g of ibuprofen within 50 ml of hexane were first placed in a high-pressure cell (100 cm³). CO₂ was pumped into the high-pressure cell through a pre-heater at pressure and temperature of 20 MPa and 333 K. The cell was then placed in an air bath and the system temperature was maintained at 333 K. The mixture was stirred with a magnetic agitator for 6 h. After each experiment, the vessel slowly depressurized to atmospheric pressure for approximately 30 min, and samples were removed. After the incorporation of ibuprofen by filtration, the remaining hexane was removed at 80°C under reduced pressure.

Characterization of the prepared MIL-53(Fe) and MIL-100(Fe)

The structure and morphology of the products were analysed using a scanning electron microscope (SEM; Elionix ERA-8900FE). The SEM samples were prepared by mounting the products on a small brass plate covered with a small piece of double-sided carbon conductive tape. The samples were then sputter coated with a silver-palladium alloy to facilitate imaging by SEM. The crystal structures of the samples were confirmed by X-ray diffraction (XRD) using Cu-K α radiation (Rigaku RAD-IIC). The BET surface areas of the porous iron (III) polycarboxylate MOFs were calculated by nitrogen sorption-desorption experiments (Micrometrics TriStar 3000). The thermal decomposition behaviour of the MOFs, ibuprofen, and ibuprofen-loaded MOFs was analysed by thermogravimetric analysis (TGA, Shimadzu TGA-50) at temperatures up to 1000 K at a heating rate of 5 K•min⁻¹ in air. The amount of ibuprofen within the MOF was also determined by TGA. In order to check the reliability of TGA measurement, the ibuprofen amount was determined by high performance liquid chromatography (HPLC), and the elemental analysis using an electron probe

microanalyzer (EPMA; Shimadzu, EPMA 1720H) equipped with a wavelength dispersive X-ray spectrometer (WDX). The mean particle diameter of MOFs was determined by a particle size analyzer (Otsuka Electronics Co., Ltd., ELSZ-1000ZS).

Dissolution test of ibuprofen from MIL-53(Fe) and MIL-100(Fe)

0.5 g of the ibuprofen-containing MIL-53(Fe) or MIL-100(Fe) was compacted by isostatic pressure (3 MPa) to obtain the disks (13 mm in diameter) used in the delivery assays. The dissolution tests were carried out by soaking the samples in 100 ml of a phosphate buffer solution (PBS, 0.05 M, pH 7.4) at 37°C under continuous stirring (100 rpm). A 1 ml aliquot of supernatant was recovered by centrifugation (5,000 rpm) at selected times throughout the experiment. The concentration of the ibuprofen was then calculated by high performance liquid chromatography (HPLC).

Conclusions

We have succeeded in the scCO_2 -assisted loading of ibuprofen on MIL-53(Fe) and MIL-100(Fe) by demonstrating the high guest loading and controlled release of these materials. The impregnation and drying procedure using scCO_2 provided greater access to the pores of the MOFs, subsequently producing larger pore volumes and a higher loading of guest molecules for drug delivery applications. The scCO_2 -assisted approach is expected to incorporate complex molecules within the pores of MOFs under mild conditions for the biological delivery of various molecules.

Acknowledgments

This work was supported by MEXT KAKENHI (25420821) and the Yoshida Science and Technology Foundation.

References

1. H.-C. Zhou, J. R. Long and O. M. Yaghi, *Chem. Rev.*, 2012, 112, 673.
2. C. M. Doherty, D. Buso, A. J. Hill, S. Furukawa, S. Kitagawa and P. Falcaro, *Acc. Chem. Res.*, 2013, 47, 396.
3. M. L. Foo, R. Matsuda and S. Kitagawa, *Chem. Mater.*, 2013, 26, 310.
4. S. T. Meek, J. A. Greathouse and M. D. Allendorf, *Adv. Mater.*, 2011, 23, 249.
5. D. Farrusseng, *Metal-Organic Frameworks: Applications from Catalysis to Gas Storage*, Wiley, 2011.
6. H. Furukawa, K. E. Cordova, M. O'Keeffe and O. M. Yaghi, *Science*, 2013, 341.
7. P. Horcajada, R. Gref, T. Baati, P. K. Allan, G. Maurin, P. Couvreur, G. Férey, R. E. Morris and C. Serre, *Chem. Rev.*, 2012, 112, 1232.
8. A. C. McKinlay, R. E. Morris, P. Horcajada, G. Férey, R. Gref, P. Couvreur and C. Serre, *Angew. Chem. Int. Ed.*, 2010, 49, 6260.
9. R. C. Huxford, J. Della Rocca and W. Lin, *Curr. Opin. Chem. Biol.*, 2010, 14, 262.
10. S. Keskin and S. Kızılel, *Ind. Eng. Chem. Res.*, 2011, 50, 1799.
11. P. Horcajada, C. Serre, M. Vallet-Regí, M. Sebban, F. Taulelle and G. Férey, *Angew. Chem. Int. Ed.*, 2006, 45, 5974.
12. P. Horcajada, T. Chalati, C. Serre, B. Gillet, C. Sebrie, T. Baati, J. F. Eubank, D. Heurtaux, P. Clayette, C. Kreuz, J. S. Chang, Y. K. Hwang, V. Marsaud, P. N. Bories, L. Cynober, S. Gil, G. Férey, P. Couvreur and R. Gref, *Nature Materials*, 2010, 9, 172.
13. P. Horcajada, C. Serre, G. Maurin, N. A. Ramsahye, F. Balas, M. Vallet-Regí, M. Sebban, F. Taulelle and G. Férey, *J. Am. Chem. Soc.*, 2008, 130, 6774.
14. S. R. Miller, D. Heurtaux, T. Baati, P. Horcajada, J. M. Grenèche and C. Serre, *Chem. Commun.*, 2010, 46, 4526.
15. M. C. Bernini, D. Fairen-Jimenez, M. Pasinetti, A. J. Ramirez-Pastor and R. Q. Snurr, *J. Mater. Chem. B*, 2014, 2, 766.
16. D. Cunha, M. Ben Yahia, S. Hall, S. R. Miller, H. Chevreau, E. Elkaïm, G. Maurin, P. Horcajada and C. Serre, *Chem. Mater.*, 2013, 25, 2767.
17. N. Liedana, P. Lozano, A. Galve, C. Tellez and J. Coronas, *J. Mater. Chem. B*, 2014, 2, 1144.
18. R. E. Morris and P. S. Wheatley, *Angew. Chem. Int. Ed.*, 2008, 47, 4966.
19. X. Lin, J. Jia, X. Zhao, K. M. Thomas, A. J. Blake, G. S. Walker, N. R. Champness, P. Hubberstey and M. Schröder, *Angew. Chem. Int. Ed.*, 2006, 45, 7358.
20. T. Düren, F. Millange, G. Férey, K. S. Walton and R. Q. Snurr, *J. Phys. Chem. C*, 2007, 111, 15350.
21. A. I. Cooper, *Adv. Mater.*, 2003, 15, 1049.
22. R. Sui and P. Charpentier, *Chem. Rev.*, 2012, 112, 3057.

23. Z. H. Xiang, D. P. Cao, X. H. Shao, W. C. Wang, J. W. Zhang and W. Z. Wu, *Chem. Eng. Sci.*, 2010, 65, 3140.
24. H. J. Park, D. W. Lim, W. S. Yang, T. R. Oh and M. P. Suh, *Chem. Eur. J.*, 2011, 17, 7251.
25. M. R. Lohe, M. Rose and S. Kaskel, *Chem. Commun.*, 2009, 6056.
26. A. P. Nelson, O. K. Farha, K. L. Mulfort and J. T. Hupp, *J. Am. Chem. Soc.*, 2009, 131, 458.
27. J. E. Mondloch, O. Karagiari, O. K. Farha and J. T. Hupp, *CrystEngComm*, 2013, 15, 9258.
28. B. Liu, A. G. Wong-Foy and A. J. Matzger, *Chem. Commun.*, 2013, 49, 1419.
29. O. K. Farha and J. T. Hupp, *Acc. Chem. Res.*, 2010, 43, 1166.
30. A. I. Cooper and M. J. Rosseinsky, *Nature Chem.*, 2009, 1, 26.
31. H. Wakayama and Y. Fukushima, *Ind. Eng. Chem. Res.*, 2005, 45, 3328.
32. Z. Y. Sun, X. R. Zhang, B. X. Han, Y. Y. Wu, G. M. An, Z. M. Liu, S. D. Miao and Z. J. Miao, *Carbon*, 2007, 45, 2589.
33. K. Matsuyama, K. Mishima, T. Kato and K. Ohara, *Ind. Eng. Chem. Res.*, 2010, 49, 8510.
34. K. Matsuyama, K. Mishima, T. Kato and K. Ohara, *J. Supercrit. Fluids*, 2011, 57, 198.
35. Y. J. Zhao, J. L. Zhang, J. L. Song, J. S. Li, J. L. Liu, T. B. Wu, P. Zhang and B. X. Han, *Green Chem.*, 2011, 13, 2078.
36. S. N. Joung, C. W. Yoo, H. Y. Shin, S. Y. Kim, K. P. Yoo, C. S. Lee and W. S. Huh, *Fluid Phase Equilib.*, 2001, 185, 219.
37. P. Horcajada, S. Surble, C. Serre, D.-Y. Hong, Y.-K. Seo, J.-S. Chang, J.-M. Greneche, I. Margiolaki and G. Ferey, *Chem. Commun.*, 2007, 2820.
38. P. G. Jessop and B. Subramaniam, *Chem. Rev.*, 2007, 107, 2666.
39. M. Charoenthaikool, F. Dehghani, N. R. Foster and H. K. Chan, *Ind. Eng. Chem. Res.*, 2000, 39, 4794.
40. M. Muntó, N. Ventosa, S. Sala and J. Veciana, *J. Supercrit. Fluids*, 2008, 47, 147.
41. A. Hillerstrom, J. van Stam and M. Andersson, *Green Chem.*, 2009, 11, 662.

Figure Captions

Fig. 1 SEM photographs of the porous iron (III)-based MOF particles. MIL-53(Fe) prepared with scCO₂ drying (a-1) and conventional vacuum drying (a-2). MIL-100(Fe) prepared with scCO₂ drying (b-1) and conventional vacuum drying (b-2).

Fig. 2 N₂ adsorption-desorption isotherms of the porous iron (III)-based MOFs. MIL-53(Fe) prepared with scCO₂ drying (a-1) and conventional vacuum drying (a-2). MIL-100(Fe) prepared with scCO₂ drying (b-1) and conventional vacuum drying (b-2).

Fig. 3 XRD patterns of the porous iron (III)-based MOF particles. MIL-53(Fe) prepared with scCO₂ drying (a-1) and conventional vacuum drying (a-2). MIL-100(Fe) prepared with scCO₂ drying (b-1) and conventional vacuum drying (b-2).

Fig. 4 TGA curves of pristine MIL-53(Fe), pristine ibuprofen, and ibuprofen-loaded MIL-53(Fe). (a): pristine MIL-53(Fe) (a-1) and ibuprofen (a-2), (b): conventional ibuprofen loading into MIL-53(Fe) prepared with conventional drying, (c): conventional ibuprofen loading into MIL-53(Fe) prepared with scCO₂ drying, (d): scCO₂-assisted ibuprofen loading into MIL-53(Fe) prepared with scCO₂ drying.

Fig. 5 TGA curves of pristine MIL-100(Fe), pristine ibuprofen, and ibuprofen-loaded MIL-100(Fe). (a): pristine MIL-100(Fe) (a-1) and ibuprofen (a-2), (b): conventional ibuprofen loading into MIL-100(Fe) prepared with conventional drying, (c): conventional ibuprofen loading into MIL-100(Fe) prepared with scCO₂ drying, (d): scCO₂-assisted ibuprofen loading into MIL-100(Fe) prepared with scCO₂ drying.

Fig. 6 FT-IR spectra of (a) pristine MIL-53(Fe), (b) pristine ibuprofen, and (c) scCO₂-assisted ibuprofen loading into MIL-53(Fe) prepared with scCO₂ drying.

Fig. 7 Ibuprofen release from MIL-53(Fe) in PBS at 25°C. (a): conventional ibuprofen loading into MIL-53(Fe) prepared with conventional drying (●), (b): conventional ibuprofen loading into MIL-53(Fe)

prepared with scCO₂ drying (▲), (c): scCO₂-assisted ibuprofen loading into MIL-53(Fe) prepared with scCO₂ drying (■).

Fig. 8 Ibuprofen release from MIL-100(Fe) in PBS at 25°C. (a): conventional ibuprofen loading into MIL-100(Fe) prepared with conventional drying (●), (b): conventional ibuprofen loading into MIL-100(Fe) prepared with scCO₂ drying (▲), (c): scCO₂-assisted ibuprofen loading into MIL-100(Fe) prepared with scCO₂ drying (■).

Table 1 BET surface area and pore volume of MIL-53(Fe) and MIL-100(Fe) by conventional vacuum and scCO₂ drying.

material	drying method	BET surface area	pore volume	mean particle	standard Dev. of
		$S_{\text{BET}}[\text{m}^2 \cdot \text{g}^{-1}]$	$V_p[\text{cm}^3 \cdot \text{g}^{-1}]$	diam. $D_p[\mu\text{m}]$	$D_p[\mu\text{m}]$
MIL-53(Fe)	vacuum drying	57	0.077	20	4.3
	scCO ₂ drying	990	0.79	0.77	0.16
MIL-100(Fe)	vacuum drying	1230	0.75	21	5.1
	scCO ₂ drying	1500	0.77	0.34	0.07

Table 2 Loading ratios of ibuprofen in MIL-53(Fe) and MIL-100(Fe) by conventional and scCO₂-assisted impregnation methods.

material	drying method	impregnation solvent	loading ratio	loading ratio	loading ratio
			determined by TGA [wt.%]	determined by elemental analysis (EPMA) [wt.%]	determined by HPLC [wt.%]
MIL-53(Fe)	vacuum drying	hexane	13.2	-	16.9
	scCO ₂ drying	hexane	15.5	-	18.3
	scCO ₂ drying	scCO ₂ +hexane	31.3	25.9	35.0
	without drying	scCO ₂ +hexane	9.0	-	-
MIL-100(Fe)	vacuum drying	hexane	6.9	-	6.6
	scCO ₂ drying	hexane	9.1	-	8.9
	scCO ₂ drying	scCO ₂ +hexane	41.7	38.9	43.4

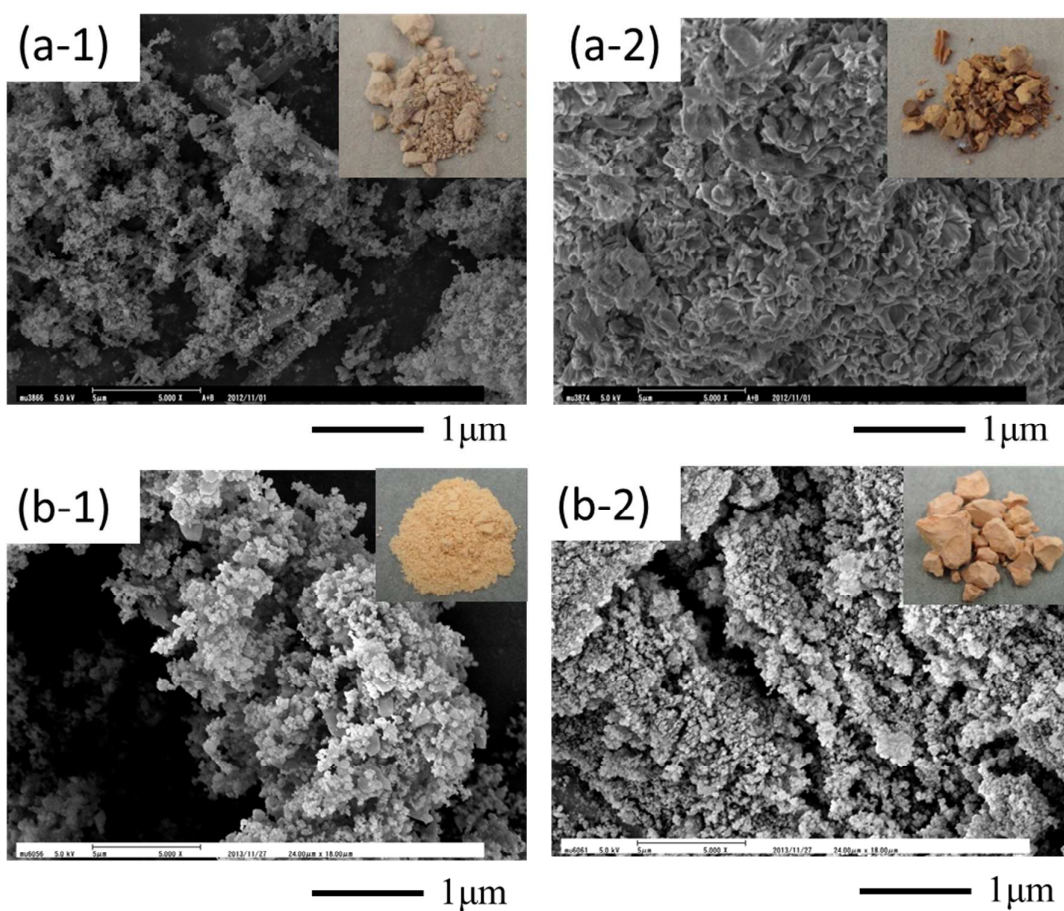


Fig. 1 SEM photographs of the porous iron (III)-based MOF particles. MIL-53(Fe) prepared with $scCO_2$ drying (a-1) and conventional vacuum drying (a-2). MIL-100(Fe) prepared with $scCO_2$ drying (b-1) and conventional vacuum drying (b-2).

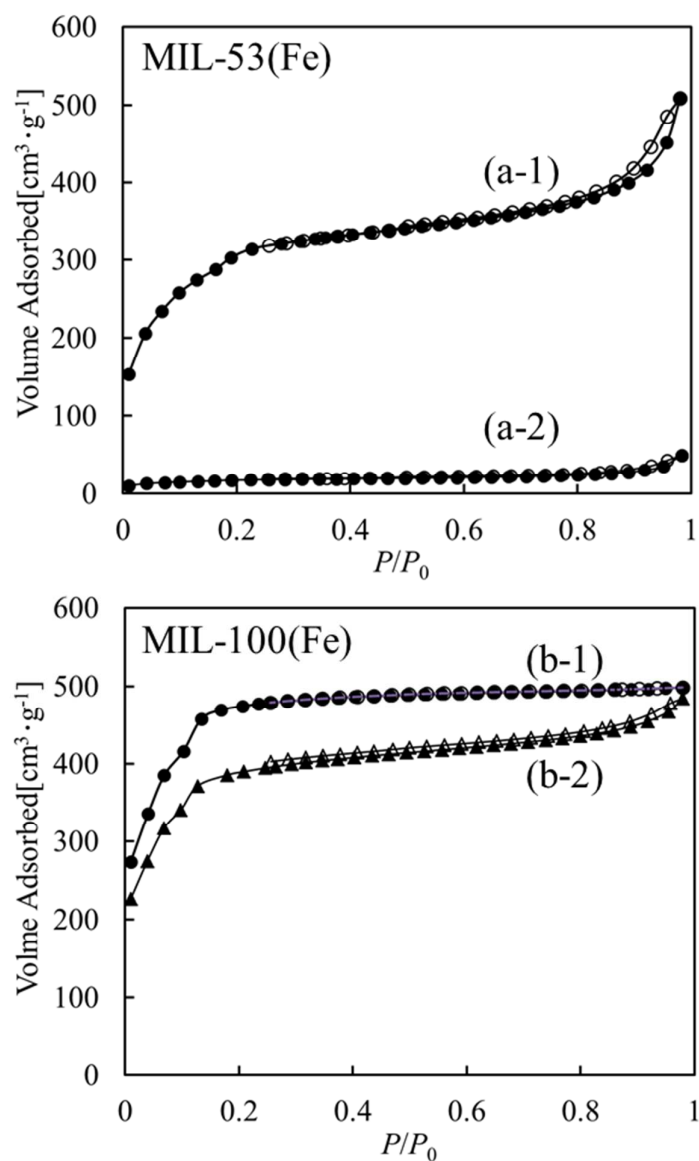


Fig. 2 N₂ adsorption-desorption isotherms of the porous iron (III)-based MOFs. MIL-53(Fe) prepared with scCO₂ drying (a-1) and conventional vacuum drying (a-2). MIL-100(Fe) prepared with scCO₂ drying (b-1) and conventional vacuum drying (b-2).

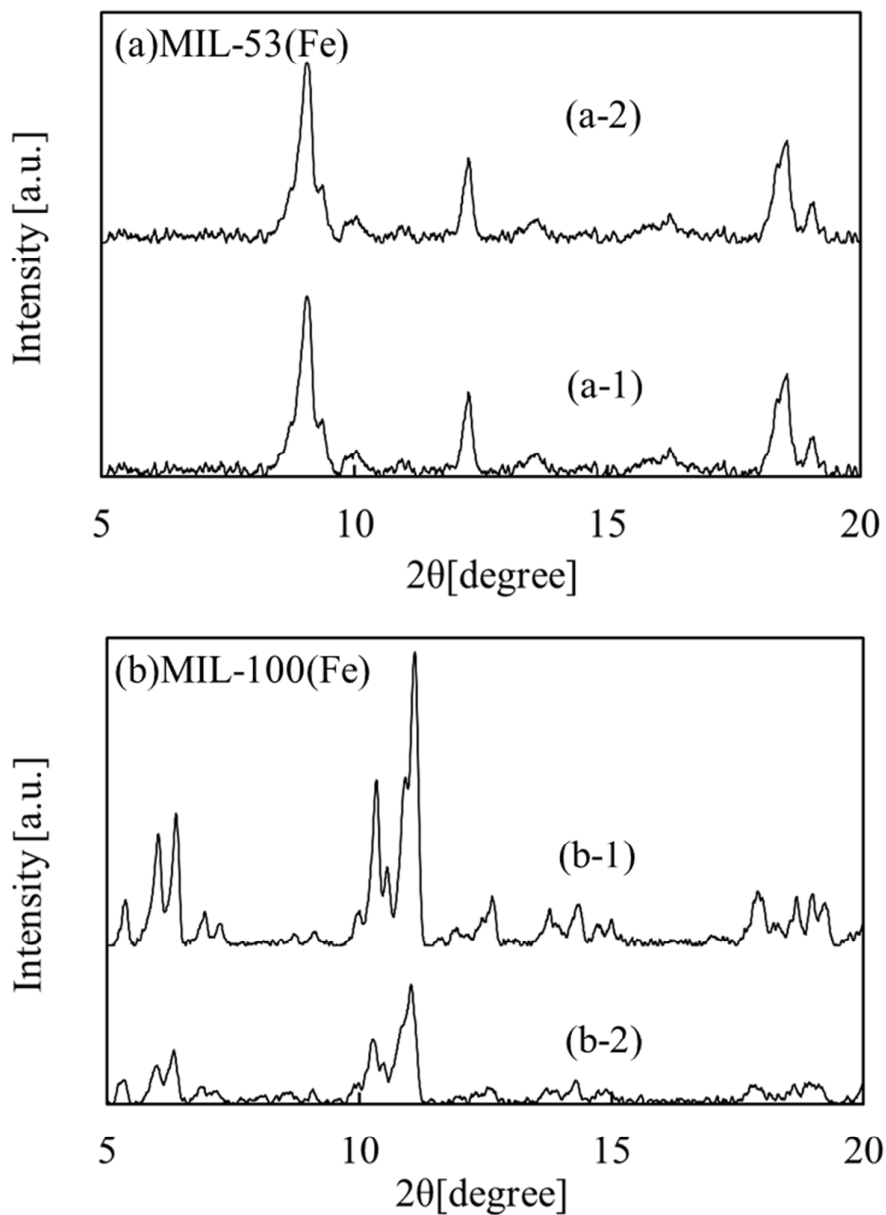


Fig. 3 XRD patterns of the porous iron (III)-based MOF particles. MIL-53(Fe) prepared with scCO_2 drying (a-1) and conventional vacuum drying (a-2). MIL-100(Fe) prepared with scCO_2 drying (b-1) and conventional vacuum drying (b-2).

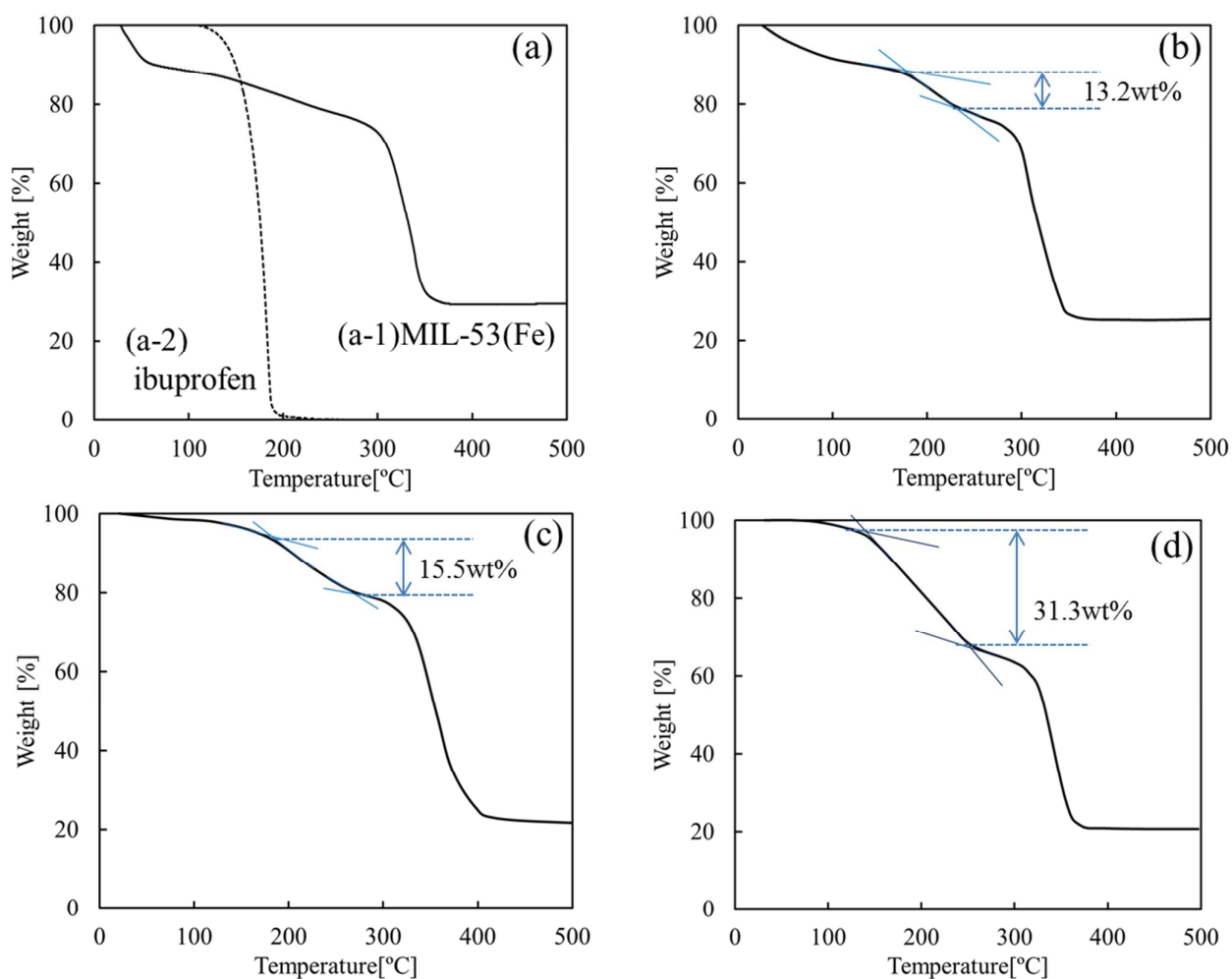


Fig. 4 TGA curves of pristine MIL-53(Fe), pristine ibuprofen, and ibuprofen-loaded MIL-53(Fe). (a): pristine MIL-53(Fe) (a-1) and ibuprofen (a-2), (b): conventional ibuprofen loading into MIL-53(Fe) prepared with conventional drying, (c): conventional ibuprofen loading into MIL-53(Fe) prepared with scCO₂ drying, (d): scCO₂-assisted ibuprofen loading into MIL-53(Fe) prepared with scCO₂ drying.

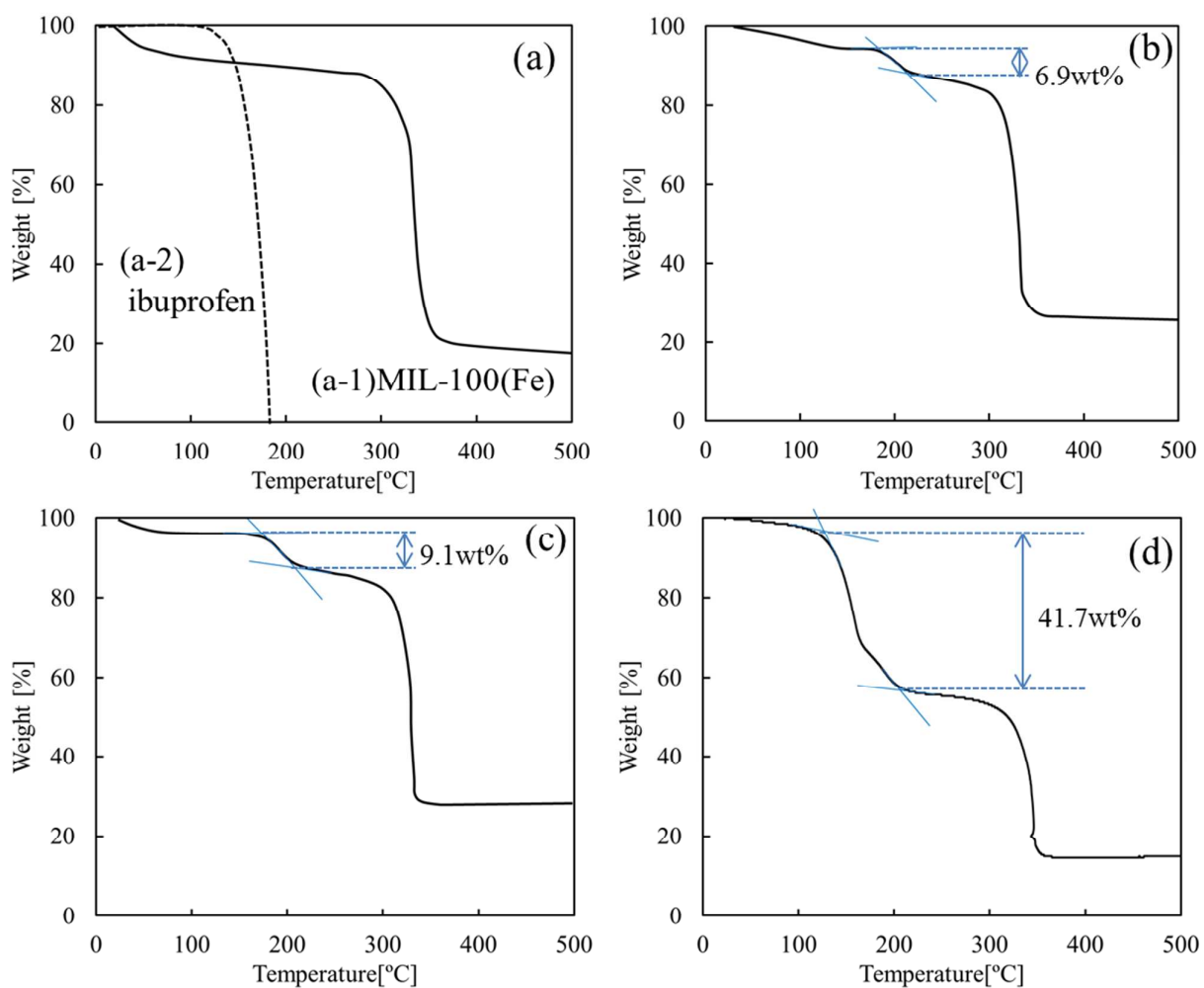


Fig. 5 TGA curves of pristine MIL-100(Fe), pristine ibuprofen, and ibuprofen-loaded MIL-100(Fe). (a): pristine MIL-100(Fe) (a-1) and ibuprofen (a-2), (b): conventional ibuprofen loading into MIL-100(Fe) prepared with conventional drying, (c): conventional ibuprofen loading into MIL-100(Fe) prepared with scCO₂ drying, (d): scCO₂-assisted ibuprofen loading into MIL-100(Fe) prepared with scCO₂ drying.

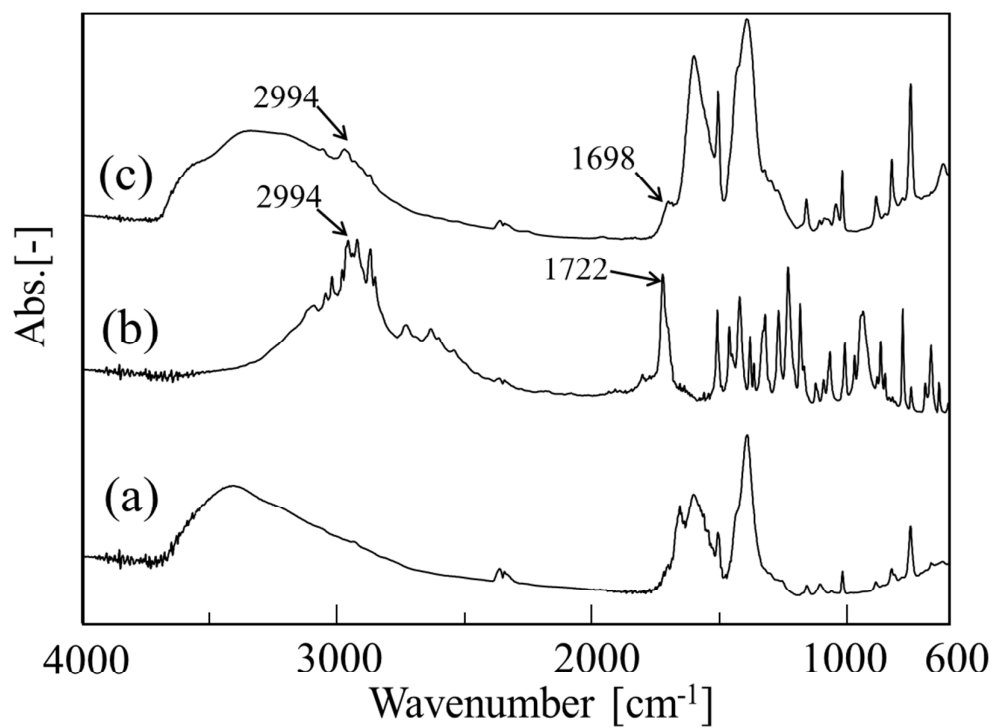


Fig. 6 FT-IR spectra of (a) pristine MIL-53(Fe), (b) pristine ibuprofen, (c) scCO₂-assisted ibuprofen loading into MIL-53(Fe) prepared with scCO₂ drying.

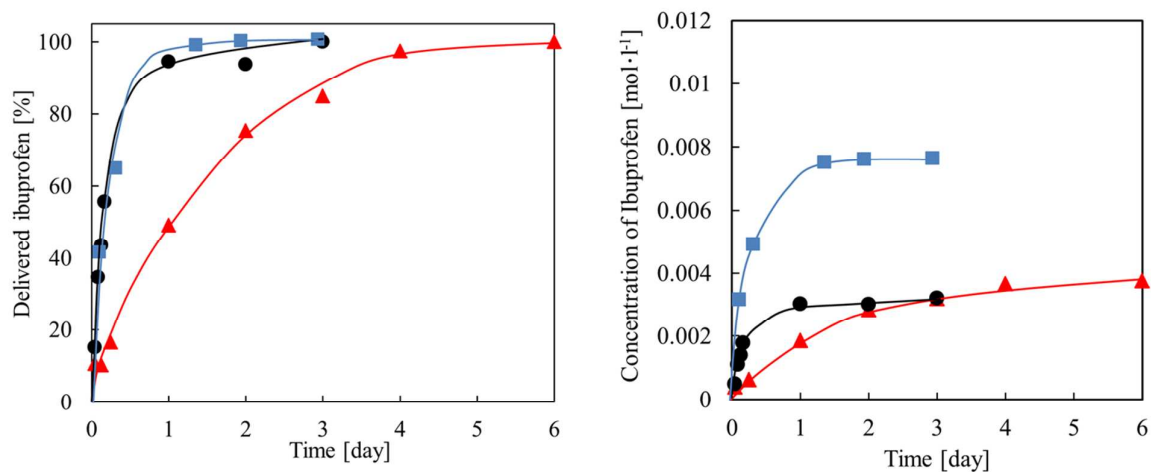


Fig. 7 Ibuprofen release from MIL-53(Fe) in PBS at 25°C. (a): conventional ibuprofen loading into MIL-53(Fe) prepared with conventional drying (●), (b): conventional ibuprofen loading into MIL-53(Fe) prepared with scCO₂ drying (▲), (c): scCO₂-assisted ibuprofen loading into MIL-53(Fe) prepared with scCO₂ drying (■).

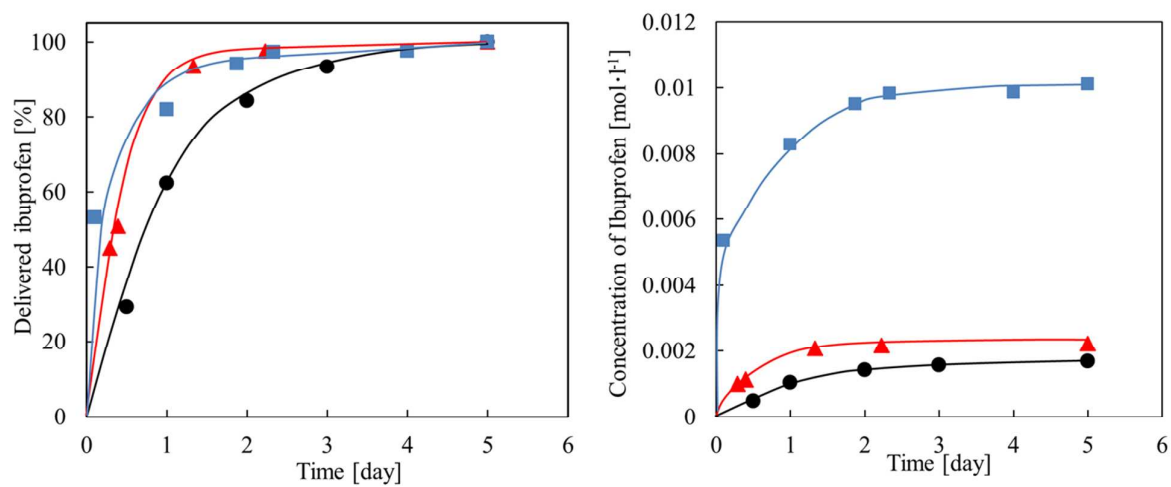


Fig. 8 Ibuprofen release from MIL-100(Fe) in PBS at 25°C. (a): conventional ibuprofen loading into MIL-100(Fe) prepared with conventional drying (●), (b): conventional ibuprofen loading into MIL-100(Fe) prepared with scCO₂ drying (▲), (c): scCO₂-assisted ibuprofen loading into MIL-100(Fe) prepared with scCO₂ drying (■).

The scCO_2 -assisted loading of ibuprofen on nontoxic and biocompatible porous iron (III) polycarboxylate metal-organic frameworks (MOFs) demonstrated the high guest loading and controlled release of these materials.

